



PAPER • OPEN ACCESS

# Positron impact excitation of lowest autoionizing state of potassium atom using distorted wave method with absorption and polarization potentials

To cite this article: Noah Nzeki William *et al* 2021 *J. Phys. Commun.* **5** 025006

View the [article online](#) for updates and enhancements.

## You may also like

- [Positronium formation for positron scattering from metastable hydrogen](#)  
Lin Lin, , Hong-Nian Wang et al.
- [Methods and progress in studying inelastic interactions between positrons and atoms](#)  
R D DuBois
- [Triple-differential cross sections for the ionization of thymine by electrons and positrons](#)  
C Dal Cappello, I Charpentier, S Houamer et al.



## PAPER

## OPEN ACCESS

RECEIVED  
22 December 2020REVISED  
21 January 2021ACCEPTED FOR PUBLICATION  
26 January 2021PUBLISHED  
25 February 2021

Original content from this work may be used under the terms of the [Creative Commons Attribution 4.0 licence](#).

Any further distribution of this work must maintain attribution to the author(s) and the title of the work, journal citation and DOI.



# Positron impact excitation of lowest autoionizing state of potassium atom using distorted wave method with absorption and polarization potentials

Noah Nzeki William<sup>1</sup> , Eric Ouma Jobunga<sup>2</sup> and Chandra Shekhar Singh<sup>1</sup> <sup>1</sup> Department of Physics, Kenyatta University, Nairobi, Kenya<sup>2</sup> Department of Mathematics and Physics, Technical University of Mombasa, Mombasa, KenyaE-mail: [noahnzeki@gmail.com](mailto:noahnzeki@gmail.com), [ejobunga@tum.ac.ke](mailto:ejobunga@tum.ac.ke) and [singh.chadra@ku.ac.ke](mailto:singh.chadra@ku.ac.ke)**Keywords:** Positron, Potassium, lowest autoionizing state, Distortion potential, Distorted wave, Cross-section

## Abstract

Differential and integral cross-sections, as well as the alignment and lambda parameters for positron impact excitation of the lowest autoionizing state of potassium atom, have been calculated using a non-relativistic distorted wave method in the energy range of 18.9–1500 eV. The distortion potential in the initial and final channel state comprises a linear combination of static potential plus polarization and absorption potentials. The approximate Roothaan-Hartree-Fock (RHF) wavefunctions Multi zeta wave functions given by Clementi and Roetti have been used. The inclusion of polarization and absorption potentials has improved integral cross-section and alignment parameter results. The integral cross sections have shown the near-threshold resonance structure revealed in electron impact excitation experimental results. Differential cross-section and lambda parameter results have been calculated and presented for future comparison since there are no other results available in the literature for positron impact excitation.

## 1. Introduction

Electron scattering from atoms and molecules has remained the focus of atomic collision physics for most of the last century. Currently, there is an increased focus on positron (anti-matter of electron) scattering from these systems. Early theoretical studies into positron-atom scattering have seen a tremendous boost with the exceptional computational power that has been available in the last three decades [1–3]. Experimental data on positron-atom scattering is also expanding with the availability of mono-energetic positron beams that were first developed by Costello *et al* [4].

Investigations of the scattering of positrons by atoms have gained significant importance because the positron being a positively-charged probe offers a more sensitive test of our ability to understand atomic interactions than the electron does [5, 6]. In recent decades, positron scattering from alkali atoms has triggered considerable involvement of both experimentalists and theoreticians due to their intriguing features such as low ionization potential and high polarizability [7, 8]. Furthermore, the alkali atoms are interesting constituents of the stellar atmosphere and other plasmas because of the presence of resonance lines in the visible or UV part of the electromagnetic spectrum [9, 10]. In addition, the alkali atoms have a comparatively simple electronic structure with the outermost shells consisting of a single electron. To a certain degree, they can be viewed as an approximate one-electron atom and can adequately be described using Hartree-Fock approximation [8, 11].

An additional importance of positron scattering derives from the fact that it involves interactions of matter with antimatter which have possible applications in the astrophysical arena [12, 13]. Moreover, positrons are crucial for the development of several applications and technological fields as discussed by Charlton and Humberston [14]. For example, in plasma science, positrons are slowed down and accumulated using the positron accumulation experiment (PAX) [15] to increase the pair plasma density in the positron-electron experiment (APEX) [16] which confines electron-positron plasmas. Also, material sciences use positron annihilation lifetime spectroscopy (PALS) to analyze

and study crystal defects [17]. Furthermore, Medical science utilizes positron emission tomography (PET) scanners in the diagnosis of cancer, heart problems, and certain brain disorders [18].

In addition to the above-mentioned applications, different numerical codes have been used for characterizing the charged particle transport in biological matter. Some examples of numerical codes used include PENELOPE (PENetration and Energy LOSS of Positrons and Electrons) [19], GEANT, GEANT3, and GEANT4 (GEometry ANd Tracking) [20]. Most of the uses of positrons discussed above depend on a quantitative understanding of the basic interactions of positrons with matter. The interaction of positrons with atoms and molecules is a cornerstone of this knowledge [6]. The positron impact scattering cross-section data over a broad energy range are thus in demand to be used in such applications and simulations [8].

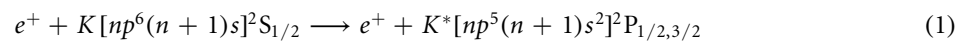
This study is stimulated by the fact that in most calculations done on the excitation of the lowest autoionizing state of potassium, an electron is used as the projectile. Also, despite the progress in positron beam experiments, no much attempt has been made in the positron impact excitation of autoionizing states of alkali atoms which is of fundamental importance. So far, there is no experimental study done on the lowest autoionizing state of potassium using positron impact excitation. On the side of theory, the only theoretical results available are for a similar study which was done by Pangantiwar and Srivastava [21] hence no other results on positron impact to compare with. It is therefore interesting to see how the use of different distortion potentials and the multi-zeta wave functions affect the results for positron impact. The availability of results for both electron and positron impact will give a better understanding of the dynamics of excitation of autoionizing state of potassium. It would also expand the results database for theoretical calculations of positron impact excitation of alkali atom.

The difficulty of the measurement of the excitation cross-section makes it necessary to develop a theoretical method reliably applicable to various collision systems [22]. The distorted wave method (DWM) has been chosen as the method of study in this case because it is a high energy approximation method that has been quite successful in explaining the various features of the excitation process. It also provides results that are in good agreement with the experimental data at intermediate and high impact energy excitation [23, 24]. The distorted wave method is less expensive computationally as compared to other reliable theories like R-matrix and close-coupling methods [24]. However, it cannot be assumed that a method appropriate for electron scattering necessarily works well for positron since in positron collisions with atoms, the exchange between particles is absent and a rearrangement channel called positronium formation is present. The alkali atoms are unique in that the positronium formation channel is open even at zero energy. This is because alkali atoms have an ionization potential that is lower than the binding energy of positronium, that is, 6.8eV [14].

## 2. Theory

### 2.1. Transition matrix

The excitation process of potassium atom by positron is shown below in equation (1) whereby an electron is excited from 3p state to 4s state.



Here, the excitation process is considered to involve one atomic electron. We treat the alkali as one-electron atoms. That is the valence electron is considered to move in a fixed effective potential (frozen-core approximation) [25]. In the distorted wave method with two-potential approach, the transition matrix for the excitation of a one-electron system from an initial state  $i$  to a final state  $f$  by the impact of the positron in the absence of exchange is given as [26];

$$T_{if} = \langle \chi_f^-(r_o) \psi_f(r_1) | V(r_o, r_1) | \chi_i^+(r_o) \psi_i(r_1) \rangle \quad (2)$$

The positron-atom interaction potential  $V(r_o, r_1)$  is given as;

$$V(r_o, r_1) = \frac{Z_p}{r_o} - \frac{Z_p}{r_{o1}} \quad (3)$$

where;  $r_o$  and  $r_1$  are the position vectors of the incident positron and atomic electron undergoing the transition relative to the target nucleus taken as the origin of the center of mass respectively.  $r_{o1}$  is the column vector between the positron and the target electron. Here  $Z_p$  is the charge of the incident particle and is taken as +1 for positron.  $\psi_i$  and  $\psi_f$  are properly anti-symmetrized initial and final atomic wave functions for the isolated atom. Roothan-Hartree-Fock (RHF) multi-zeta atomic wave functions as given in the Clementi and Roetti [27] tables were used in order to evaluate the transition matrix outlined above in equation (2). A multi-zeta function is an approximate RHF function in which a given electron orbital is described by many slater functions [27].

$\chi_i$  and  $\chi_f$  in equation (2) are the scattered positron distorted wave functions in the initial and final channels respectively with the wave vectors  $k_i$  and  $k_f$ . The distorted wave functions can be obtained by solving the following equations:

$$\left(\frac{1}{2}\nabla_o^2 + U_i - \frac{1}{2}\mathbf{k}_i^2\right)\chi_i^+ = 0 \quad (4)$$

$$\left(\frac{1}{2}\nabla_o^2 + U_f - \frac{1}{2}\mathbf{k}_f^2\right)\chi_f^- = 0 \quad (5)$$

Here the (+) and (−) superscript indicates the outgoing and incoming wave boundary conditions respectively.  $U_i$  and  $U_f$  are the distorting potentials in the initial and final channels respectively. The distortion potentials are clearly discussed in the next section.

To evaluate the scattering amplitude, the distorted waves  $\chi_i^+$  and  $\chi_f^-$  shown in equations (4), (5) are first expanded in terms of partial waves [26] as follows:

$$|\chi_i^+\rangle = \sqrt{\frac{2}{\pi}} \frac{1}{k_i r} \sum_{l_i m_i} i^{l_i} \chi_{l_i}(k_i, r) Y_{l_i}^{m_i}(\hat{r}) Y_{l_i}^{m_i*}(\hat{k}_i) \quad (6)$$

$$|\chi_f^-\rangle = \sqrt{\frac{2}{\pi}} \frac{1}{k_f r} \sum_{l_f m_f} i^{l_f} \chi_{l_f}^*(k_i, r) Y_{l_f}^{m_f}(\hat{r}) Y_{l_f}^{m_f*}(\hat{k}_f) \quad (7)$$

Here,  $Y_l^m$ 's are spherical harmonics. In the expansion of equation (7) the radial distorted wave is taken as a complex conjugate so that it satisfies the incoming wave boundary conditions. Using equations (6) and (7) in (4) and (5) respectively, it is seen that the radial distorted waves are solutions of the differential equation:

$$\left(\frac{d^2}{dr^2} - \frac{l_s(l_s + 1)}{r^2} - U_s(r) + k_s^2\right)\chi_{l_s}(r) = 0 \quad (8)$$

The radial distorted wave equations are solved by using the Numerov's method [26]. Here  $s = i$  for the initial state and  $s = f$  for the final state distorted waves. In the asymptotic region, they satisfy the boundary condition;

$$\lim_{r \rightarrow \infty} \chi_{l_s}(k_s, r) = j_{l_s} + \alpha_l(-\eta_{l_s} + i j_{l_s}) \quad (9)$$

here,  $j_l$  and  $\eta_l$  are regular and irregular Ricatti-Bessel functions [28], while  $\alpha_l = \exp(i\delta_l)\sin(\delta_l)$  where  $\delta_l$  is the elastic scattering phase shift.

## 2.2. Distortion potentials

In this study, the full distortion potential for positron and electron impact excitation in both channels is given by equations (10), (11) below respectively,

$$U_{i/f} = V_{i/f}^{st}(r) + V^{pol}(r) + iV^{abs}(r) \quad (10)$$

$$= V_{i/f}^{st}(r) + V^{pol}(r) + iV^{abs}(r) + V^{exc}(r) \quad (11)$$

With the distortion potential in this form, the distorted-wave functions given in equations (4), (5) incorporates in it the distortion of the projectile by the static field of the target, distortion due to the polarization of the target, and the effect of contribution due to the absorption of incident projectile flux from the channels. It also takes into account the effect of the exchange of the projectile electron with the bound electrons of the target atom (for electron impact excitation).

In the initial channel distortion potential, the static potential ( $V_i^{st}(r)$ ) is taken as the static potential of the target atom in its initial state while in the final channel distortion potential  $V_f^{st}(r)$  is a simple average of target atom static potentials in its initial and final states [29]. That is;

$$V_i^{st}(r) = \langle \psi_i | V | \psi_i \rangle \quad (12)$$

$$V_f^{st}(r) = \frac{1}{2} \langle \psi_i | V | \psi_i \rangle + \frac{1}{2} \langle \psi_f | V | \psi_f \rangle \quad (13)$$

The reason for taking the above choice is that when the projectile positron is in its initial state, it sees' the initial state static potential of the target atom for all the time it is in its field. However, when the energy of the projectile positron is transferred to the target atom, it takes time (relaxation time) for the atom to go to its final state. That is, there is a time lag between the time of transfer of energy and the instant when the atom reaches the final state. Thus, the projectile in its final state sees' a potential which is intermediate between the initial and final-state static potentials of the target [29].

The static potential of the target atom is obtained by averaging over the motion of the target electrons written as [30];

$$V^{st}(r_o) = \frac{Ze_p}{r_o} - \sum_{i=1}^Z e_p \int |\Psi(r_1, r_2 \dots, r_Z)|^2 \times \frac{1}{|r_o - r_i|} dr_1 \dots dr_Z \quad (14)$$

where;  $Z$  is the nuclear charge of the target atom and  $e_p$  is the projectile charge.  $\Psi(r_1, r_2 \dots, r_Z)$  is the antisymmetrized Hartree–Fock wave function of the target and is expanded in terms of the Slater-type orbitals:

$$\Phi_{\lambda p} = \sum_{i=1}^M A(\lambda, p, i) r^{n(p,i)-1} \exp[-\zeta(p, i)r] Y_l^m(\hat{r})$$

$$\equiv \phi_{\lambda p}(r) Y_l^m(\hat{r}) \quad (15)$$

with,

$$A(\lambda, p, i) = C(\lambda, p, i) \{2[n(p, i)]!\}^{-1/2} [2\zeta(p, i)]^{n(p,i)+1/2}$$

Here,  $C(\lambda, p, i)$ ,  $\zeta(p, i)$  and  $n(p, i)$  represent the orbital expansion coefficient, orbital exponents of multi-zeta function, and principal quantum number for the given orbital respectively. Their values were obtained from the table of basis functions and their coefficients by Clementi and Roetti [27]. The basis functions  $\phi_{\lambda p}(r)$  in equation (15) are slater orbital with the radial component. The static potential is thus given by the relation [30];

$$V^{st}(r) = e_p \sum_{\lambda=1}^N \sum_{p=0}^{\lambda-1} N_{\lambda p} \sum_{i=1}^M \sum_{j=1}^M a \exp(-zr) \left[ \frac{s}{r} + \sum_{t=0}^{v-2} m r^t \right] \quad (16)$$

Here;

$$\begin{aligned} v &= n(p, i) + n(p, j), \\ z &= \zeta(p, i) + \zeta(p, j), \\ a &= A(\lambda, p, i) A(\lambda, p, j) v!, \\ s &= z^{-v-1} \text{ and} \\ m &= \frac{1/(t+1)! - 1/(t!v)}{z^{v-t}} \end{aligned}$$

where;  $i, j$ , and  $t$  are integers.  $N$  is the number of occupied shells in the atom and  $N_{\lambda p}$  is the number of electrons in the orbital  $(\lambda, p)$ .  $M$  in equation (16) is the number of slater orbitals obtained from Clementi and Roetti [27] tables.

The model of absorption potential used in this study is based on the quasifree-scattering model with Pauli blocking. The absorption potential for impact energy  $E$  at a point  $\vec{r}$  is as shown below [31];

$$V^{abs}(\vec{r}, E) = \frac{1}{2} U_{loc} \rho(r) \bar{\sigma}_b \quad (17)$$

where;  $U_{loc}(\vec{r}, E) = [2(E - V^{SE})]^{1/2}$  is the local speed of the incident projectile,  $\rho(r)$  is the electron charge density of the target atom and  $V^{SE}(\vec{r}, E)$  is the static plus exchange potential (for positron impact there is no exchange).  $\bar{\sigma}_b(\vec{r}, E)$  is the average binary collision cross-section obtained by averaging the Rutherford cross-sections (with a semi-classical correction factor  $\frac{1}{2}$  that approximately accounts for the effect of exchange) over a free electron gas of density  $\rho(r)$  subject to the constraints.

$$(k')^2 \geq \alpha \quad (18)$$

$$(p')^2 \geq \beta \quad (19)$$

where  $k'$  and  $p'$  are the final momenta of the target electron and the projectile particle after the collision. The constraints provided by equations (18), (19) on  $k'$  and  $p'$  were chosen to account for the Pauli exclusion principle. The average binary collision cross-section has the below-mentioned form [31].

$$\bar{\sigma}_b(\vec{r}, E) = \begin{cases} \frac{32\pi^2 N_k}{15p^2} (f_1 + f_2), & p^2 \geq \alpha + \beta - k_F^2; \\ 0, & p^2 < \alpha + \beta - k_F^2 \end{cases} \quad (20)$$

where,

$$\begin{aligned} N_k(\vec{r}) &= \frac{3}{4\pi k_F^2} \\ p(E) &= (2E)^{1/2} \\ f_1(\vec{r}, E) &= \frac{5k_F^2}{(\alpha - k_F^2)} - \frac{k_F^3 [5(p^2 - \beta) + 2k_F^2]}{(p^2 - \beta)^2} \\ f_2(\vec{r}, E) &= \begin{cases} 0, & p^2 > \alpha + \beta \\ \frac{2(\alpha + \beta - p^2)^{5/2}}{(p^2 - \beta)^2}, & p^2 \leq \alpha + \beta \end{cases} \\ k_F(\vec{r}) &= (3\pi^2 \rho)^{1/3} \\ \alpha(\vec{r}, E) &= k_F^2 + 2\Delta \\ \beta(\vec{r}, E) &= k_F^2 \end{aligned}$$

The quantities  $N_k(\vec{r})$  and  $k_F$  are the momentum state density per target electron and Fermi wave number (or momentum) corresponding to the target electron density  $\rho$  respectively.  $\Delta$  is the energy gap between the target

ground-state energy and the final energy of the originally bound target electron.  $V^{abs}(\vec{r}, E)$  must be zero below it and a non zero above it. It is considered to be the positronium formation threshold ( $E_{ps}$ ). In the case of positron scattering from alkali-metal atoms  $E_{ps}$  is zero and in order to apply the quasi-free model to positron scattering from alkali-metal atoms, we set  $\Delta$  equal to the lowest non-zero inelastic threshold, which is the excitation thresholds for our target. The appropriate value for our target is,  $\Delta = 1.62$  eV [32]. The absorption potential takes into account various inelastic processes such as positronium formation as well as excitation and ionization of the target by positron impact [5]. The polarization potential used is of Buckingham type used by Nahar and Wadehra [30] and it takes the form;

$$V^{pol}(r) = \frac{-\alpha_d r^2}{2(r^2 + d^2)^3} \quad (21)$$

Where  $\alpha_d$  is the static dipole polarizability of the atom and  $d$  is the energy-dependent adjustable parameter. For neutral potassium atom,  $\alpha_d = 289.7a_0^3$  as given by Schwerdtfeger and Nagle [33]. Energy-dependent adjustable parameter was used at some low impact energies. The  $d$  values were determined by fitting the present electron impact excitation integral cross-sections with the electron impact excitation experimental values at a particular energy. The same value of  $d$  was then used for positron impact excitation calculations at that energy. The polarization potential describes the behavior of the target atom when the projectile is within the interaction region [34]

For the electron impact excitation calculations in this work, a semi-classical exchange potential of (Furness and McCarthy) [35] given below was used:

$$V^{exc}(r) = \frac{1}{2}[E - V^{st}(r)] - \frac{1}{2}\{[E - V^{st}(r)]^2 + 4\pi a_0 \varepsilon_0 e^4 \rho(r)\}^{1/2} \quad (22)$$

which is directly derived from the formal expression of the non-local exchange interaction by using a WKB-like approximation for the wave functions. Here  $a_0$  is the Bohr radius and  $E$  is the incident electron energy.

### 2.3. Cross-sections and angular correlation parameters

The differential cross-sections summed over the magnetic sub levels are obtained using the relation;

$$\left(\frac{d\sigma}{d\Omega}\right)_{3p \rightarrow 4s} = 4\pi^4 \frac{k_f}{k_i} \sum_{m=-1}^1 |T_{3p \rightarrow 4s}|^2 \quad (23)$$

The angle-resolved differential cross-sections ( $\sigma'_m(\theta, \phi)$ ) are related to their scattering amplitude ( $f_m(\theta, \phi)$ ) as given below;

$$\sigma'_m(\theta, \phi) = \frac{k_f}{k_i} |f_m(\theta, \phi)|^2 \quad (24)$$

with the scattering amplitude directly connected to the transition matrix using the relation [26];

$$f_m(\theta, \phi) = -2\pi^2 T_{if}(m) \quad (25)$$

The total cross-sections ( $\sigma$ ) are the probability of scattering per unit incident flux and are obtained by summing differential cross sections at all solid angles as shown in the relation below;

$$\sigma = \int_0^{2\pi} \int_0^\pi \frac{d\sigma}{d\Omega} \sin \theta d\theta d\phi \quad (26)$$

For high impact energies, a sufficient number of partial waves were used to ensure that the cross-sections are well converged.

Angular correlation parameters between the scattered positron when the atom is excited from  $np \rightarrow (n+1)s$  state and the emitted photon from transition  $(n+1)s \rightarrow np$  after excitation, are determined in order to obtain details regarding the population of magnetic sub-states. Compared to the integral and differential cross-sections, the study of angular correlation parameters provides a much deeper and more detailed insight into the dynamics of atomic collision processes [36]. The lambda parameter ( $\lambda$ ) is important in predicting the phases of the amplitude of different scattering angles and it is calculated using the relation [37];

$$\lambda = \frac{\sigma'_0(\theta, \phi)}{\sigma'_0(\theta, \phi) + 2\sigma'_1(\theta, \phi)}, 0 \leq \lambda \leq 1 \quad (27)$$

where,  $\sigma'_0(\theta, \phi)$  and  $\sigma'_1(\theta, \phi)$  are the differential cross sections for transition with  $m = 0$  and  $m = 1$  respectively. The anisotropy parameter  $\beta$  or the  $A_2$  alignment parameter of the autoionizing excited state  $A^*[np^5(n+1)s^2]P_{1/2,3/2}$  is such that;  $\beta = A_2 = -A_{20}$  [38]

$$A_{20} = \frac{\sigma(np_1) - \sigma(np_0)}{\sigma(np_0) + 2\sigma(np_1)} \quad (28)$$

Here,  $\sigma(np_m)$  is the total cross-section of an  $np_m$  electron excited to a  $(n + 1)s$  state

### 3. Results and discussion

In this study, the distorted wave method has been used to calculate integral cross sections, differential cross sections, alignment parameter, and lambda parameter for positron impact excitation of the lowest autoionizing state of potassium ( $3p^5 4s^2$ )<sup>2</sup>P. A non-relativistic Schrödinger equation that does not resolve the fine structure effects was solved. The calculations were done for positron impact energies ranging from 18.9 eV to 1500 eV for different distorting potentials. That is, static potential only, static plus absorption potentials, static plus polarization potentials, and static plus absorption plus polarization potentials. For the sake of meaningful comparison, we calculated electron impact excitation results for all the parameters. In the present electron impact excitation results we used a distorting potential which comprised of; static, absorption, polarization, and exchange potentials. Our results are compared amongst themselves and with experimental and theoretical results available in the literature where applicable.

#### 3.1. Integral cross-sections

The present integral cross sections for positron impact excitation of the lowest autoionizing state of the potassium atom are calculated using different distorting potentials as given in table 1. Present electron impact

**Table 1.** Present integral cross-section results in  $\pi a_0^2$  for positron (using different distortion potentials) and electron impact excitation of the lowest autoionizing state of potassium.

Energy (eV)	PP-S ( $e^+$ )	PP-SA ( $e^+$ )	PP-SP ( $e^+$ )	PP-SPA + ( $e^+$ )	PE-SPA $e^-$
18.90	1.6120E-04	7.2570E-04	1.4540E-02	1.1130E-02	2.9000E-03
18.95	2.4660E-04	8.0350E-04	2.3330E-02	1.8550E-02	3.9400E-03
19.00	3.2440E-04	8.1700E-04	1.7900E-02	1.4710E-02	4.5400E-03
19.10	4.9580E-04	2.5000E-03	1.1770E-02	1.1390E-02	6.1700E-03
19.20	6.8700E-04	2.2700E-03	9.5300E-03	7.5700E-03	5.0000E-03
19.30	8.7280E-04	1.8700E-03	8.6100E-03	7.2600E-03	5.9000E-03
19.40	1.0900E-03	4.0200E-03	8.3700E-03	1.2350E-02	1.0990E-02
19.50	1.2900E-03	3.7500E-03	8.7000E-03	6.6600E-03	7.8800E-03
19.70	1.7600E-03	2.7600E-03	1.1930E-02	1.0280E-02	4.0250E-02
19.90	2.2300E-03	4.4800E-03	2.5310E-02	2.2080E-02	1.8840E-01
20.00	2.4900E-03	3.7800E-03	4.5930E-02	4.1940E-02	1.9930E-01
20.10	2.7300E-03	6.3400E-03	1.0200E-01	6.4140E-02	2.5960E-02
20.50	3.7800E-03	7.1200E-03	1.8020E-01	1.5660E-01	4.1040E-02
20.60	4.0400E-03	6.2900E-03	1.3330E-01	1.2620E-01	4.6930E-02
21.00	5.1500E-03	6.8000E-03	8.5110E-02	5.9690E-02	3.0820E-02
22.00	7.9500E-03	1.1200E-02	4.4620E-02	7.3000E-03	5.1500E-03
25.00	1.5970E-02	1.4410E-02	3.3240E-02	2.9360E-02	2.4350E-02
30.00	2.6460E-02	2.4540E-02	4.5030E-02	4.1960E-02	3.7120E-02
40.00	3.8570E-02	3.6570E-02	4.5350E-02	4.3040E-02	3.8040E-02
50.00	4.3910E-02	4.2210E-02	4.0370E-02	3.9010E-02	3.6380E-02
60.00	4.6020E-02	4.4620E-02	5.0310E-02	4.8870E-02	4.6240E-02
70.00	4.6510E-02	4.5350E-02	5.2570E-02	5.1250E-02	4.8320E-02
80.00	4.6080E-02	4.5130E-02	4.5400E-02	4.4520E-02	4.1010E-02
90.00	4.5270E-02	4.4480E-02	4.4240E-02	4.3520E-02	4.2040E-02
100.0	4.4240E-02	4.3570E-02	4.4660E-02	4.3990E-02	4.2690E-02
110.0	4.3100E-02	4.2530E-02	4.5170E-02	4.4400E-02	4.3210E-02
120.0	4.1800E-02	4.1310E-02	4.4290E-02	4.3130E-02	4.1800E-02
150.0	3.8090E-02	3.7770E-02	3.3570E-02	3.3290E-02	3.2730E-02
200.0	3.4020E-02	3.4020E-02	3.3260E-02	3.3190E-02	3.2800E-02
250.0	3.0400E-02	3.0360E-02	2.9020E-02	2.8930E-02	2.8340E-02
300.0	2.7510E-02	2.7480E-02	2.6890E-02	2.6860E-02	2.6650E-02
400.0	2.3150E-02	2.3130E-02	2.2750E-02	2.2730E-02	2.2520E-02
500.0	1.9990E-02	1.9980E-02	1.9810E-02	1.9790E-02	1.9710E-02
700.0	1.5620E-02	1.5620E-02	1.5510E-02	1.5500E-02	1.5460E-02
1000.0	1.1490E-02	1.1480E-02	1.1500E-02	1.1500E-02	1.1470E-02
1500.0	7.5500E-03	7.5500E-03	7.5800E-03	7.5800E-03	7.5700E-03

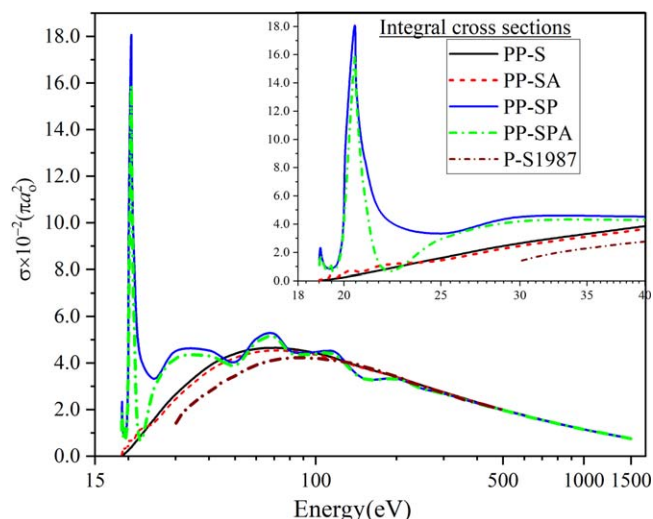


**Figure 1.** Integral cross-section results for positron impact excitation of lowest autoionizing state of potassium. PP-S—Present positron impact excitation results using static potential only; PP-SA—Present positron impact excitation results using static and absorption potentials; PP-SP—Present positron impact excitation results using static and polarization potentials; PP-SPA—Present positron impact excitation results using static, polarization, and absorption potentials; P-S1987—Positron impact excitation results of Pangantiwar and Srivastava [21].

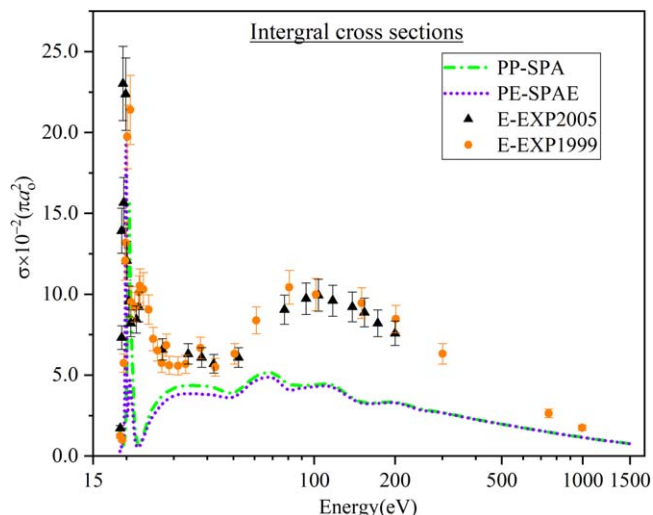
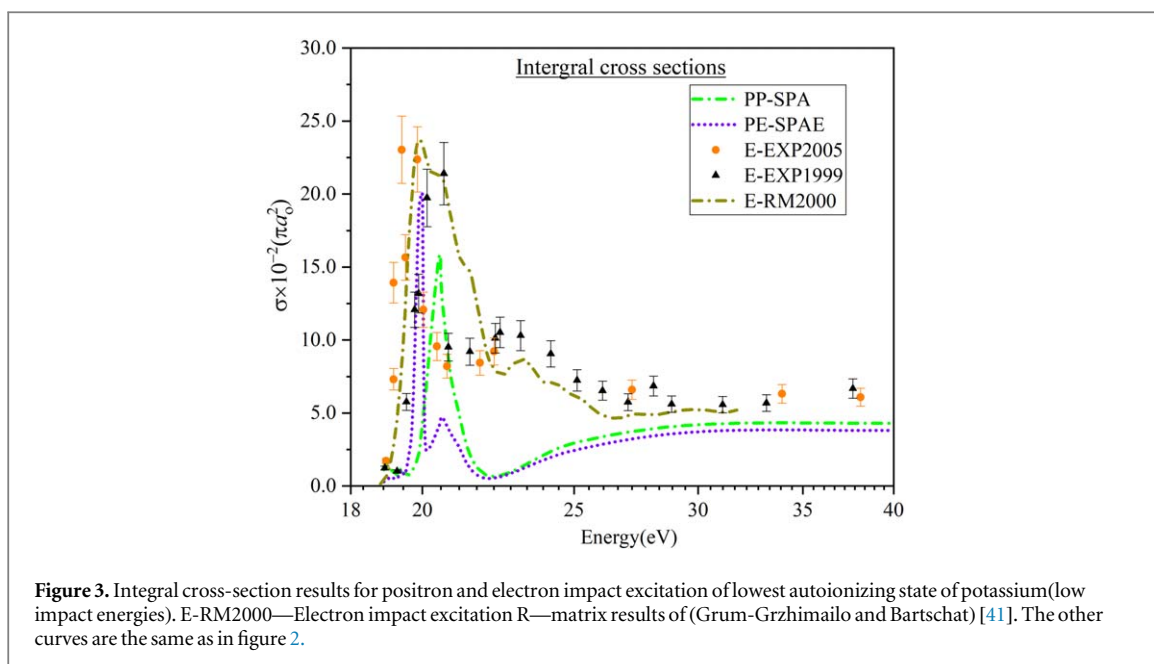


**Figure 2.** Integral cross-section results for positron and electron impact excitation of lowest autoionizing state of potassium. PP-SPA—Present positron impact excitation results using static, polarization, and absorption; PE-SPA—Present electron impact excitation results; E-EXP1999—Electron impact excitation experimental results of Feuerstein *et al* [39]; E-EXP2005—Electron impact excitation experimental results of Borovik *et al* [40].

excitation results are also included for comparison. In each case, the energy of the projectile varies from the near excitation threshold to 1500 eV. In figure 1 present positron impact excitation integral cross-sections are compared amongst themselves and with the only available theoretical results of Pangantiwar and Srivastava [21]. In figures 2, 3 our positron impact excitation results using static, polarization, and absorption potentials are compared with present electron impact excitation results and electron impact excitation experimental results of Feuerstein *et al* [39] and Borovik *et al* [40]. Also, our results at low impact energies have been compared with electron impact excitation R—matrix results of (Grum-Grzhimailo and Bartschat) [41] as shown in figure 3.

The present integral cross-section results using static potential only are in good qualitative agreement with Pangantiwar and Srivastava [21] results. The disparity at low and intermediate energies is attributed to the choice of distorting potential. In the present calculation, a simple average of target atom static potentials in its initial and final states is used in the final channel where else Pangantiwar and Srivastava [21] used the static potential of the target in final states for the final channel.



The effect of absorption was noted at low impact energies near the excitation threshold. After which there is an insignificant difference in magnitude compared with the results using static potential only. This is because inelastic processes such as positronium formation as well as excitation and ionization of the target have a contribution to the integral cross sections at low impact energies. In fact, positronium formation in potassium has a maximum about 5 eV and above about 20 eV its contribution to cross-sections is negligible [42]. As mentioned above results for impact energies below the excitation threshold because the approximation method used in this study is not accurate at these energies.

Using a distortion potential with static and polarization potential produced results that have sharp resonance structure near the excitation threshold. The resonance shows an increased probability of interaction in this energy region. This implies that the behavior of the target as the projectile approaches (polarization) has a high contribution to the integral cross sections in this energy region. Positron impact excitation integral cross-section results using a distorting potential with static potential, polarization potential, and absorption potential have the same resonance behavior near the excitation threshold. The results had a slight difference at low impact energies but the difference in magnitude is insignificant at intermediate and high energies compared to the results when using static and polarization potentials. This confirms that the effect of absorption potential is negligible on our results at intermediate and high energies.

The effect of polarization potential seen in positron impact excitation results was also seen in electron impact excitation results. This is because polarization potential is attractive and of the same magnitude for both positrons and electrons [14]. The present electron excitation results exhibited the same resonance structure near the excitation threshold. The sharp peak in the integral cross sections results is because the cross-sections are dominated by a strong negative-ion core-excited  $3p^5 3d4s^2$  resonance of  $^3F^o$  symmetry, slightly above the excitation threshold [41]. The polarization potential used affects the electron impact excitation integral cross-section results at low energies bringing them closer to the electron impact experimental results [39, 40] and electron impact excitation R—matrix results [41]. Although, there is a disparity in terms of magnitude in the energy region 20 eV to around 25 eV. This is because the non-relativistic method used is not very accurate at low impact energies to fully describe the resonance structure near the excitation threshold. From this comparison with electron impact excitation experimental, we can say that the positron impact excitation experimental results (if done in the future) will not have a big deviation (qualitatively) from our results.

Comparing the present electron impact excitation results and the present positron impact excitation results using static, polarization, and absorption potentials, both the results have the same trend as shown in figures 2, 3. The slight difference in terms of magnitude noted at low impact energies is possibly due to projectile electron-target electron exchange interaction which has a substantial effect on the results within this energy region. A slight shift of the peak of the positron impact excitation integral cross-section curve to higher incident energies relative to electron impact excitation results is also noted. At intermediate (from about 30.0 eV) and high energies, the electron impact excitation results have no substantial difference from the positron impact excitation results and the curves have the same trend. This is because exchange and absorption potentials which

take into account the differences between the two projectiles have no significant effect on integral cross sections in this energy region [39, 40, 42].

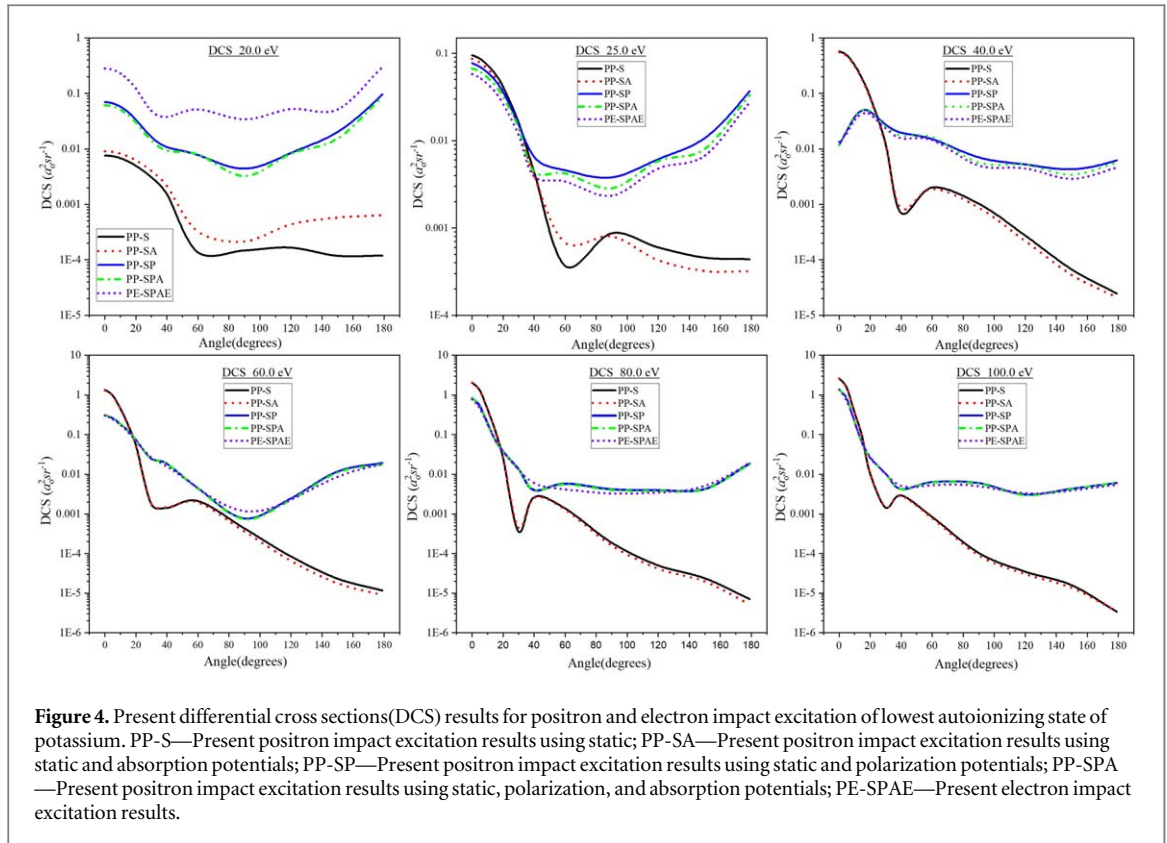
At high energies the effect of absorption and polarization potentials is negligible and the cross-sections using the different distortion potentials are nearly equal. This is due to less interaction between the projectile positron and the target atom thus the potentials do not have substantial time for their effects to manifest. The magnitude of the integral cross sections at high energies is decreasing because the projectile passes the target without much effect reducing the collision time which in turn decreases the interaction probability. The convergence of our present integral cross-sections with the electron impact experimental results is slow as shown in figure 2. This was expected because the single configuration Hartree–Fock model used in this study predicts energy levels which are not highly accurate for the lowest states [25].

### 3.2. Differential cross-sections

In addition to integral cross-sections, we have calculated differential cross sections for positron impact energies 20.0, 25.0, 40.0, 60.0, 80.0 and 100.0 eV using different distortion potentials as presented in table 2. As in the integral cross-section, present electron impact excitation results for the same energies have also been included

**Table 2.** Present differential cross-section results in  $a_0^2 \text{sr}^{-1}$  for positron (using different distortion potentials) and electron impact excitation of the lowest autoionizing state of potassium.

20.0 eV						25.0 eV					
Energy (eV)	PP-S ( $e^+$ )	PP-SA ( $e^+$ )	PP-SP ( $e^+$ )	PP-SPA + ( $e^+$ )	PE-SPAEE- ( $e^-$ )	Energy (eV)	PP-S ( $e^+$ )	PP-SA ( $e^+$ )	PP-SP ( $e^+$ )	PP-SPA + ( $e^+$ )	PE-SPAEE- ( $e^-$ )
0	7.5000E-03	9.0000E-03	6.9930E-02	6.0660E-02	2.8111E-01	0	9.4970E-02	8.6140E-02	7.6910E-02	6.7180E-02	5.7540E-02
5	7.3200E-03	8.7900E-03	6.6920E-02	5.8050E-02	2.6723E-01	5	8.7050E-02	7.8720E-02	7.0860E-02	6.1670E-02	5.2490E-02
10	6.7700E-03	8.1900E-03	5.8600E-02	5.0870E-02	2.2924E-01	10	7.3280E-02	6.5970E-02	6.0720E-02	5.2650E-02	4.4400E-02
15	5.9300E-03	7.2500E-03	4.6930E-02	4.0820E-02	1.7682E-01	15	5.8210E-02	5.2160E-02	4.9690E-02	4.3030E-02	3.6020E-02
20	4.9500E-03	6.1500E-03	3.4450E-02	3.0130E-02	1.2246E-01	20	4.1410E-02	3.6840E-02	3.6940E-02	3.1940E-02	2.6480E-02
30	3.0900E-03	4.0100E-03	1.5700E-02	1.4250E-02	4.8550E-02	30	1.6320E-02	1.4310E-02	1.6300E-02	1.4170E-02	1.1740E-02
40	1.5200E-03	2.1400E-03	9.7400E-03	9.3300E-03	3.7720E-02	40	4.3900E-03	3.9500E-03	5.0200E-03	4.4200E-03	3.9100E-03
60	1.3650E-04	3.2142E-04	8.7200E-03	7.9300E-03	5.1200E-02	60	3.6779E-04	6.7652E-04	4.8200E-03	4.2100E-03	3.4000E-03
90	1.4666E-04	2.1320E-04	3.0700E-03	3.2400E-03	3.3930E-02	90	8.6608E-04	7.9927E-04	3.1000E-03	2.8400E-03	2.3400E-03
120	1.6417E-04	4.3369E-04	9.1700E-03	8.1100E-03	5.2060E-02	120	5.9715E-04	4.2726E-04	6.6600E-03	5.8100E-03	4.7700E-03
150	1.1707E-04	5.7344E-04	1.6520E-02	1.5290E-02	5.1290E-02	150	4.5604E-04	3.2058E-04	8.7500E-03	8.0300E-03	6.7000E-03
179	1.1783E-04	6.3212E-04	9.5540E-02	8.6090E-02	2.9818E-01	179	4.3677E-04	3.1865E-04	3.7120E-02	3.3240E-02	2.7470E-02
40.0 eV						60.0 eV					
Energy (eV)	PP-S ( $e^+$ )	PP-SA ( $e^+$ )	PP-SP ( $e^+$ )	PP-SPA + ( $e^+$ )	PE-SPAEE- ( $e^-$ )	Energy (eV)	PP-S ( $e^+$ )	PP-SA ( $e^+$ )	PP-SP ( $e^+$ )	PP-SPA + ( $e^+$ )	PE-SPAEE- ( $e^-$ )
0	5.7298E-01	5.5016E-01	1.1880E-02	1.1770E-02	1.3400E-02	0	1.3462E+00	1.3165E+00	3.0895E-01	3.0683E-01	3.0356E-01
5	4.8934E-01	4.6909E-01	2.0810E-02	2.0060E-02	1.9100E-02	5	9.9261E-01	9.6923E-01	2.6066E-01	2.5818E-01	2.5266E-01
10	3.2654E-01	3.1181E-01	3.9750E-02	3.7990E-02	3.2860E-02	10	4.6491E-01	4.5206E-01	1.8738E-01	1.8494E-01	1.7725E-01
15	1.8158E-01	1.7243E-01	5.1740E-02	4.9570E-02	4.2660E-02	15	1.7669E-01	1.7086E-01	1.2498E-01	1.2330E-01	1.1675E-01
20	8.6570E-02	8.1660E-02	4.9830E-02	4.7940E-02	4.2040E-02	20	5.5270E-02	5.3160E-02	7.4620E-02	7.3710E-02	6.9690E-02
30	1.2440E-02	1.1670E-02	2.6280E-02	2.5410E-02	2.3350E-02	30	1.7700E-03	1.8100E-03	2.4720E-02	2.4360E-02	2.3490E-02
40	6.9667E-04	8.3683E-04	1.7960E-02	1.7190E-02	1.5500E-02	40	1.4000E-03	1.4400E-03	1.8440E-02	1.8000E-02	1.7160E-02
60	1.9900E-03	1.8900E-03	1.7080E-02	1.6220E-02	1.4370E-02	60	2.0900E-03	1.9300E-03	4.4700E-03	4.3400E-03	4.2700E-03
90	1.0200E-03	8.6751E-04	5.9800E-03	5.5900E-03	4.9800E-03	90	4.2589E-04	3.5884E-04	7.6401E-04	7.3017E-04	7.4240E-04
120	2.7382E-04	2.1843E-04	5.5100E-03	5.1600E-03	4.4200E-03	120	8.3499E-05	6.4916E-05	2.4500E-03	2.2600E-03	2.0600E-03
150	6.6697E-05	5.3188E-05	3.6600E-03	3.4200E-03	2.8800E-03	150	2.3065E-05	1.7681E-05	1.1620E-02	1.0910E-02	1.0110E-02
179	2.4671E-05	2.1034E-05	6.2200E-03	5.6900E-03	4.5600E-03	179	1.1580E-05	8.7843E-06	1.9180E-02	1.7950E-02	1.7860E-02
80.0 eV						100.0 eV					
Energy (eV)	PP-S ( $e^+$ )	PP-SA ( $e^+$ )	PP-SP ( $e^+$ )	PP-SPA + ( $e^+$ )	PE-SPAEE- ( $e^-$ )	Energy (eV)	PP-S ( $e^+$ )	PP-SA ( $e^+$ )	PP-SP ( $e^+$ )	PP-SPA + ( $e^+$ )	PE-SPAEE- ( $e^-$ )
0	2.0681E+00	2.0379E+00	8.3816E-01	8.3028E-01	7.8709E-01	0	2.6462E+00	2.6176E+00	1.3935E+00	1.3835E+00	1.3693E+00
5	1.3276E+00	1.3066E+00	5.3780E-01	5.3224E-01	5.0531E-01	5	1.5237E+00	1.5059E+00	8.1023E-01	8.0398E-01	7.9459E-01
10	4.4213E-01	4.3325E-01	1.9529E-01	1.9306E-01	1.8531E-01	10	3.6730E-01	3.6139E-01	2.1753E-01	2.1552E-01	2.1170E-01
15	1.2783E-01	1.2462E-01	7.3720E-02	7.3030E-02	7.1870E-02	15	8.7530E-02	8.5710E-02	6.0390E-02	5.9740E-02	5.8150E-02
20	2.6280E-02	2.5510E-02	3.7500E-02	3.7200E-02	3.6990E-02	20	1.0530E-02	1.0300E-02	2.6290E-02	2.5970E-02	2.5590E-02
30	3.5382E-04	4.4318E-04	1.3700E-02	1.3480E-02	1.2870E-02	30	1.4300E-03	1.4700E-03	1.0410E-02	1.0330E-02	1.0180E-02
40	2.6200E-03	2.5600E-03	3.9800E-03	4.0200E-03	4.8600E-03	40	2.8900E-03	2.8100E-03	4.1900E-03	4.1600E-03	3.9100E-03
60	1.3700E-03	1.2600E-03	5.7300E-03	5.5400E-03	4.2200E-03	60	8.3774E-04	7.7585E-04	6.2500E-03	6.0900E-03	5.7600E-03
90	1.8669E-04	1.5777E-04	4.1300E-03	3.9800E-03	3.0400E-03	90	1.0233E-04	8.8553E-05	5.9300E-03	5.7600E-03	5.5300E-03
120	4.9810E-05	4.1139E-05	3.9300E-03	3.8300E-03	3.4900E-03	120	3.4667E-05	3.0188E-05	3.0400E-03	2.9600E-03	2.8500E-03
150	2.3575E-05	1.9512E-05	4.2400E-03	4.1300E-03	3.9600E-03	150	1.5723E-05	1.3463E-05	4.2400E-03	4.1800E-03	3.8700E-03
179	7.0379E-06	5.1833E-06	1.8350E-02	1.8090E-02	1.9810E-02	179	3.4073E-06	3.4427E-06	5.9900E-03	6.0000E-03	5.4200E-03



for comparison. Since there are no other results available in the literature for positron impact excitation, our differential cross-section results have been compared amongst themselves and presented in figure 4 which may be useful for future works on the same process.

The present positron impact excitation results using static potential only are characterized by a high value at small scattering angles after which the values decrease with an increase in scattering angle across all the impact energies. The effect of absorption potential on the magnitude of differential cross sections is more pronounced at low impact energies. When compared to the results using static potential only, our results using static and absorption potentials have the same trend despite the differences in magnitude at low impact energies.

The inclusion of polarization potential increases the magnitude of differential cross sections at low impact energies compared to the results using static potential only. This shows that the behavior of the target atom in response to the field of the incoming projectile (polarization) has a contribution to the cross-sections. The cross-sections have the highest values at angles  $0^\circ$  and  $180^\circ$  with a minimum value at around  $90^\circ$  as shown by the results of impact energy 20.0 eV. Since the differential cross-section is a measure of the probability of scattering in a particular direction, this indicates that the incident projectile has high chances of scattering at small angles and large angles. At intermediate and high energies, polarization potential lowers the cross-sections at small angles and gradually increases the cross-sections for angles from about  $40^\circ$  and above.

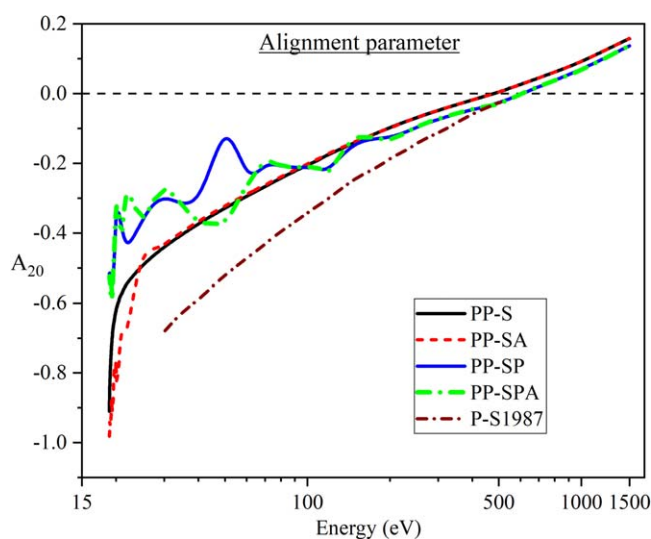
When using a distortion potential with static, polarization, and absorption potentials, the effect of polarization is dominant and the results have a small deviation from the results when using static and polarization potentials at low energies. The present electron impact excitation differential cross sections are close to our positron impact excitation results using static, polarization, and absorption potentials at all impact energies. The effect of polarization potential in positron impact excitation results is also exhibited in electron impact excitation results. At 20.0 eV, the electron impact excitation results are higher than the positron impact excitation results. This is attributed to projectile electron-target electron exchange interaction which has a significant effect on the results at low impact energies.

### 3.3. Alignment parameter

The present alignment parameter results using positron impact excitation are evaluated for different distorting potential as presented in table 3. Electron impact excitation results were also calculated for comparison purposes. In figure 5 the present results are compared with positron impact excitation results of Pangantiwar and Srivastava [21]. Present alignment parameter results using static potential only as distortion potential have the same trend as the results of Pangantiwar and Srivastava [21] though our results are slightly higher at low and intermediate energies. The difference can be attributed to the choice of distortion potential. That is, the use of a

**Table 3.** Present alignment parameter results for positron and electron impact excitation of the lowest autoionizing state of potassium.

Energy (eV)	PP-S ( $e^+$ )	PP-SA ( $e^+$ )	PP-SP ( $e^+$ )	PP-SPA + ( $e^+$ )	PE-SPA $e^-$
18.90	-9.0972E-01	-9.8151E-01	-5.1717E-01	-5.2380E-01	-5.7106E-01
18.95	-8.6685E-01	-9.6148E-01	-5.1359E-01	-5.1696E-01	-5.6288E-01
19.00	-8.2949E-01	-9.3726E-01	-5.2014E-01	-5.2159E-01	-5.6423E-01
19.10	-7.7740E-01	-9.5294E-01	-5.3580E-01	-5.7267E-01	-5.9711E-01
19.20	-7.4406E-01	-9.2428E-01	-5.4727E-01	-5.4987E-01	-5.6748E-01
19.30	-7.1201E-01	-8.7315E-01	-5.5224E-01	-5.4528E-01	-5.5015E-01
19.40	-6.9421E-01	-9.1036E-01	-5.4906E-01	-5.9093E-01	-5.5031E-01
19.50	-6.7348E-01	-8.8495E-01	-5.3522E-01	-5.2193E-01	-4.3010E-01
19.70	-6.4992E-01	-7.8967E-01	-4.7131E-01	-4.4554E-01	-3.6288E-01
19.90	-6.2876E-01	-8.1862E-01	-3.8554E-01	-3.6145E-01	-3.3638E-01
20.00	-6.2305E-01	-7.6510E-01	-3.5393E-01	-3.4111E-01	-3.3907E-01
20.10	-6.1394E-01	-8.2213E-01	-3.3509E-01	-3.2378E-01	-3.5929E-01
20.50	-5.9217E-01	-7.7522E-01	-3.4345E-01	-3.3960E-01	-3.9223E-01
20.60	-5.8592E-01	-7.3989E-01	-3.5307E-01	-3.5604E-01	-3.8951E-01
21.00	-5.7207E-01	-6.8746E-01	-3.8842E-01	-4.0340E-01	-4.2119E-01
22.00	-5.4391E-01	-6.6690E-01	-4.5420E-01	-2.8911E-01	-2.9794E-01
25.00	-4.9363E-01	-4.7672E-01	-3.5488E-01	-3.5453E-01	-3.5330E-01
30.00	-4.4071E-01	-4.3206E-01	-2.7343E-01	-2.7644E-01	-2.7800E-01
40.00	-3.7405E-01	-3.6696E-01	-3.6345E-01	-3.6451E-01	-3.6428E-01
50.00	-3.2885E-01	-3.2277E-01	-4.0370E-02	-3.6340E-01	-3.6365E-01
60.00	-2.9473E-01	-2.8939E-01	-2.6548E-01	-2.6620E-01	-2.7188E-01
70.00	-2.6729E-01	-2.6255E-01	-1.9680E-01	-1.9793E-01	-2.0313E-01
80.00	-2.4302E-01	-2.3877E-01	-2.0777E-01	-2.0760E-01	-2.0825E-01
90.00	-2.2272E-01	-2.1889E-01	-2.1248E-01	-2.1175E-01	-2.1260E-01
100.0	-2.0547E-01	-2.0201E-01	-2.1127E-01	-2.1030E-01	-2.1135E-01
110.0	-1.9016E-01	-1.8704E-01	-2.1519E-01	-2.1394E-01	-2.1526E-01
120.0	-1.7446E-01	-1.7160E-01	-2.2295E-01	-2.2039E-01	-2.2069E-01
150.0	-1.3991E-01	-1.3770E-01	-1.2827E-01	-1.2842E-01	-1.2978E-01
200.0	-9.7850E-02	-9.8610E-02	-1.3102E-01	-1.3066E-01	-1.3283E-01
250.0	-6.9780E-02	-6.9390E-02	-9.6500E-02	-9.6520E-02	-9.3160E-02
300.0	-4.8740E-02	-4.8440E-02	-7.2860E-02	-7.2510E-02	-7.3270E-02
400.0	-1.8580E-02	-1.8400E-02	-4.5250E-02	-4.5000E-02	-4.3740E-02
500.0	4.2800E-03	4.4100E-03	-2.9140E-02	-2.8820E-02	-2.9050E-02
700.0	4.4760E-02	4.4840E-02	2.0110E-02	2.0290E-02	1.9730E-02
1000.0	9.1950E-02	9.2000E-02	6.7790E-02	6.7920E-02	6.7750E-02
1500.0	1.5788E-01	1.5791E-01	1.3705E-01	1.3715E-01	1.3692E-01

**Figure 5.** Alignment parameter results for positron impact excitation of lowest autoionizing state of potassium. PP-S—Present positron impact excitation results using static potential only; PP-SA—Present positron impact excitation results using static and absorption potentials; PP-SP—Present positron impact excitation results using static and polarization potentials; PP-SPA—Present positron impact excitation results using static, polarization, and absorption potentials; P-S1987—Positron impact excitation results of Pangantiwar and Srivastava [21].

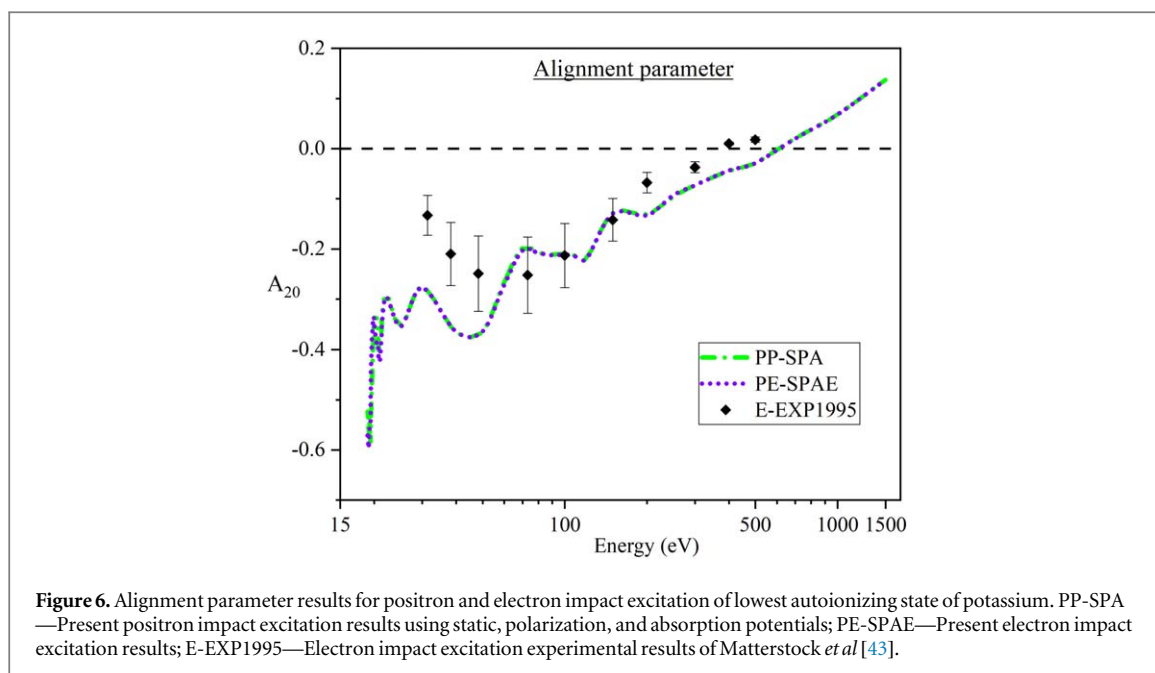


**Figure 6.** Alignment parameter results for positron and electron impact excitation of lowest autoionizing state of potassium. PP-SPA—Present positron impact excitation results using static, polarization, and absorption potentials; PE-SPA—Present electron impact excitation results; E-EXP1995—Electron impact excitation experimental results of Matterstock *et al* [43].

simple average of the target atom static potentials in its initial and final states in the final channel in the present calculation, where else Pangantiwar and Srivastava [21] used the static potential of the target in the final state for the final channel.

The effect of inclusion of absorption potential in our distortion potential is seen at low impact energies. As discussed in integral cross-section results, this is the energy region where the inclusion of absorption potential energy has a visible effect on the results. The alignment parameter results using static and absorption potentials are slightly lower than the results when using static potential only at low energy. A distortion potential with static and polarization potentials produces alignment parameter results that are higher than the results when using static potential only at low and intermediate impact energy. Resonance behavior is also shown near the excitation threshold for the present results using static and polarization potentials. Our results using static, polarization, and absorption potentials have the same trend as the results when using static and polarization potentials though there is a small variation at low energies. At high impact energies, polarization potential has no significant effect on the results. This because of the small-time of interaction which is not sufficient for the potential to show its effect.

In figure 6, our positron impact excitation results using static, polarization, and absorption potentials are compared with present electron impact excitation results and electron impact excitation experimental results of Matterstock *et al* [43]. Our positron impact excitation results are close to the present electron impact excitation results. The slight difference at low energies was expected because of the change in projectile charge. The effect of polarization potential in positron impact excitation results is also exhibited in the present electron impact excitation results. This makes the present electron impact excitation results move closer to electron impact excitation experimental results of Matterstock *et al* [43]. The disparity at high impact energies is to the poor structure model of the autoionizing state  $(3p^5 4s^2)^2P$  and neglect of the contribution of the transitions from other excited states to the lowest autoionizing level of the potassium atom. From the comparison with the electron impact excitation experimental results, we can say that the positron impact excitation experimental results (when done) will not have a large deviation from the present results.

From the formula of alignment parameter, when  $A_{20}$  is negative,  $\sigma_o$  is greater than  $\sigma_1$ . This implies that most of the excitations take place from the magnetic sub-state  $m = 0$ . When  $A_{20}$  is positive,  $\sigma_1$  is greater than  $\sigma_o$  and most of the excitations take place from  $m = 1$  magnetic sub-state. In our study, the alignment parameter is negative from above the excitation threshold up to around 500 eV as shown in figure 5. This indicates that most of the incident positrons are scattered from the magnetic sub-state  $m = 0$  in this energy range, compared to magnetic sub-state  $m = 1$ .

### 3.4. Lambda parameter

Lambda parameter results for positron impact excitation using different distorting potentials were evaluated for impact energies 20.0, 25.0, 40.0, 60.0, 80.0 and 100.0 eV as presented in table 4. Just like in the case of differential cross-sections, there are no other results of lambda parameter using positron impact excitation

**Table 4.** Present Lambda parameter results for positron (using different distortion potentials) and electron impact excitation of the lowest autoionizing state of potassium.

20.0 eV						25.0 eV					
Energy (eV)	PP-S ( $e^+$ )	PP-SA ( $e^+$ )	PP-SP ( $e^+$ )	PP-SPA + ( $e^+$ )	PE-SPA $e^-$	Energy (eV)	PP-S ( $e^+$ )	PP-SA ( $e^+$ )	PP-SP ( $e^+$ )	PP-SPA + ( $e^+$ )	PE-SPA $e^-$
0	1.0000E+00	1.0000E+00	1.0000E+00	1.0000E+00	1.0000E+00	0	1.0000E+00	1.0000E+00	1.0000E+00	1.0000E+00	1.0000E+00
5	9.9498E-01	9.9584E-01	9.8014E-01	9.7900E-01	9.7704E-01	5	9.8260E-01	9.8113E-01	9.7805E-01	9.7819E-01	9.7631E-01
10	9.8027E-01	9.8375E-01	9.1836E-01	9.1374E-01	9.0483E-01	10	9.3172E-01	9.2568E-01	9.1461E-01	9.1539E-01	9.0797E-01
15	9.5621E-01	9.6431E-01	8.0835E-01	7.9792E-01	7.7330E-01	15	8.5150E-01	8.3781E-01	8.1694E-01	8.1936E-01	8.0423E-01
20	9.2215E-01	9.3750E-01	6.4201E-01	6.2455E-01	5.6800E-01	20	7.4719E-01	7.2233E-01	6.9330E-01	6.9893E-01	6.7594E-01
30	8.1977E-01	8.6093E-01	2.0523E-01	1.9589E-01	7.2040E-02	30	4.8473E-01	4.2827E-01	3.8477E-01	3.9979E-01	3.7539E-01
40	6.6651E-01	7.6149E-01	3.5482E-01	3.7738E-01	6.8141E-01	40	1.7426E-01	1.0842E-01	7.6430E-02	8.1520E-02	9.7990E-02
60	8.5480E-02	5.8598E-01	5.2027E-01	5.0566E-01	4.3893E-01	60	9.9896E-01	9.9228E-01	8.0930E-01	8.3240E-01	8.4723E-01
90	6.5342E-01	8.1360E-01	8.6413E-01	8.7432E-01	9.9888E-01	90	7.2110E-02	1.6187E-01	5.1981E-01	5.1379E-01	5.1815E-01
120	3.2530E-02	6.9229E-01	5.4381E-01	5.2790E-01	4.4910E-01	120	1.9870E-01	1.4402E-01	4.4388E-01	4.3257E-01	4.3988E-01
150	4.3080E-01	9.0304E-01	2.5983E-01	2.4382E-01	4.6080E-02	150	7.6688E-01	7.6810E-01	9.7340E-02	9.7070E-02	9.6850E-02
179	9.9932E-01	9.9989E-01	9.9938E-01	9.9936E-01	9.9910E-01	179	9.9974E-01	9.9975E-01	9.9861E-01	9.9859E-01	9.9858E-01

40.0 eV						60.0 eV					
Energy (eV)	PP-S ( $e^+$ )	PP-SA ( $e^+$ )	PP-SP ( $e^+$ )	PP-SPA + ( $e^+$ )	PE-SPA $e^-$	Energy (eV)	PP-S ( $e^+$ )	PP-SA ( $e^+$ )	PP-SP ( $e^+$ )	PP-SPA + ( $e^+$ )	PE-SPA $e^-$
0	1.0000E+00	1.0000E+00	1.0000E+00	1.0000E+00	1.0000E+00	0	1.0000E+00	1.0000E+00	1.0000E+00	1.0000E+00	1.0000E+00
5	9.2910E-01	9.2708E-01	5.2093E-01	5.0179E-01	4.7721E-01	5	8.2567E-01	8.2277E-01	6.2446E-01	6.2326E-01	6.1783E-01
10	7.5566E-01	7.4841E-01	5.9013E-01	5.6922E-01	5.0584E-01	10	5.1774E-01	5.0934E-01	4.4514E-01	4.4214E-01	4.3173E-01
15	5.5147E-01	5.3762E-01	8.2558E-01	8.1657E-01	7.9490E-01	15	2.7995E-01	2.6708E-01	5.6779E-01	5.6407E-01	5.6913E-01
20	3.5845E-01	3.3806E-01	9.1698E-01	9.1441E-01	9.1409E-01	20	1.1741E-01	1.0221E-01	5.9080E-01	5.8592E-01	6.0420E-01
30	5.9870E-02	3.9270E-02	6.2584E-01	6.2441E-01	6.1931E-01	30	9.3930E-02	1.4733E-01	3.8683E-01	3.9374E-01	4.0308E-01
40	5.1180E-01	6.1508E-01	4.6588E-01	4.6611E-01	4.7258E-01	40	2.3192E-01	2.8409E-01	5.9214E-01	5.9364E-01	5.8913E-01
60	1.0072E-01	1.2716E-01	7.2963E-01	7.3145E-01	7.2746E-01	60	8.7700E-03	7.7900E-03	1.6758E-01	1.6191E-01	1.6830E-01
90	3.6130E-02	2.9240E-02	2.1286E-01	2.1622E-01	2.2740E-01	90	3.7190E-02	4.2270E-02	7.1033E-01	6.8456E-01	6.2245E-01
120	1.8839E-01	2.0771E-01	3.8270E-02	3.9060E-02	3.3950E-02	120	5.3620E-02	5.5260E-02	7.0121E-01	6.9809E-01	7.3183E-01
150	4.8017E-01	5.2713E-01	1.5722E-01	1.5759E-01	1.6107E-01	150	4.0223E-01	3.9403E-01	7.1501E-01	7.1714E-01	7.3287E-01
179	9.9855E-01	9.9878E-01	9.9590E-01	9.9576E-01	9.9572E-01	179	9.9404E-01	9.9296E-01	9.8477E-01	9.8471E-01	9.8593E-01

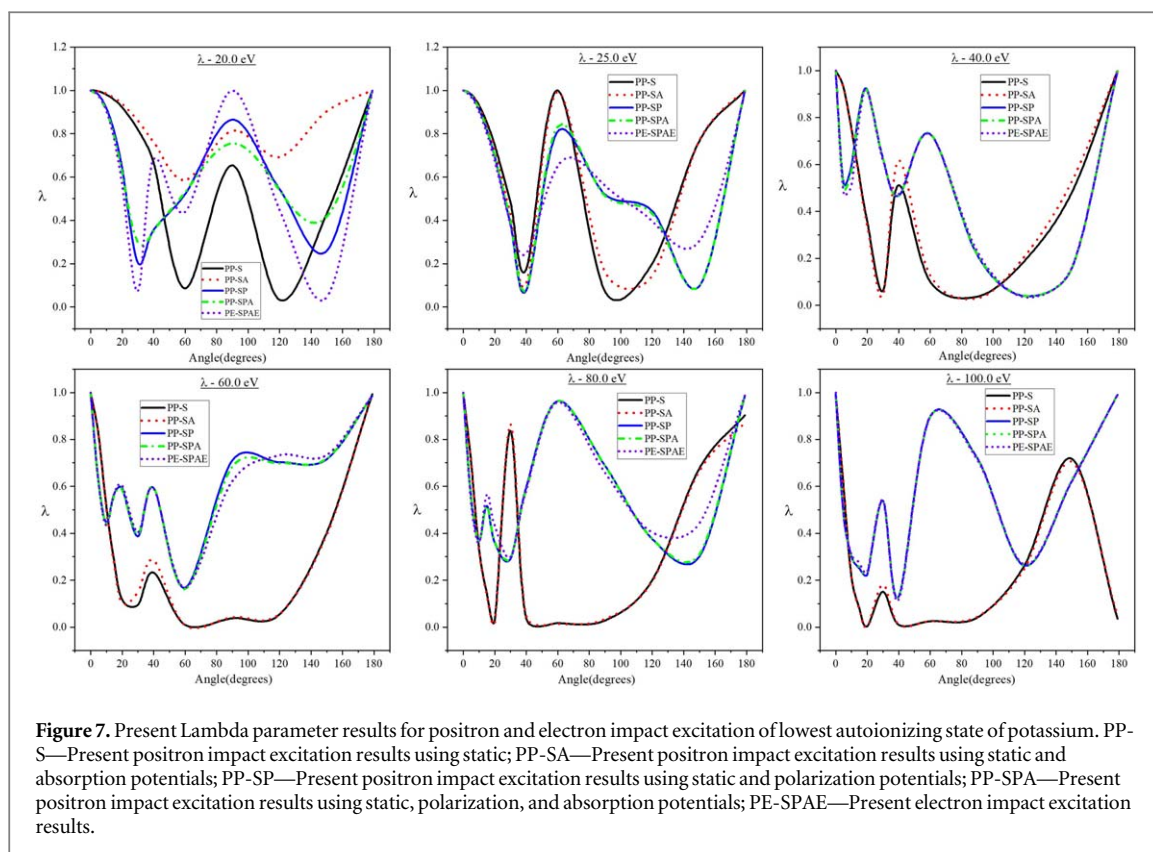
  

80.0 eV						100.0 eV					
Energy (eV)	PP-S ( $e^+$ )	PP-SA ( $e^+$ )	PP-SP ( $e^+$ )	PP-SPA + ( $e^+$ )	PE-SPA $e^-$	Energy (eV)	PP-S ( $e^+$ )	PP-SA ( $e^+$ )	PP-SP ( $e^+$ )	PP-SPA + ( $e^+$ )	PE-SPA $e^-$
0	1.0000E+00	1.0000E+00	1.0000E+00	1.0000E+00	1.0000E+00	0	1.0000E+00	1.0000E+00	1.0000E+00	1.0000E+00	1.0000E+00
5	7.1086E-01	7.0767E-01	5.5748E-01	5.5459E-01	5.3382E-01	5	6.0555E-01	6.0244E-01	4.8625E-01	4.8382E-01	4.8179E-01
10	3.3991E-01	3.3230E-01	3.6607E-01	3.6348E-01	3.5723E-01	10	2.1917E-01	2.1277E-01	3.0217E-01	3.0148E-01	3.0942E-01
15	1.4533E-01	1.3550E-01	5.1626E-01	5.1748E-01	5.6514E-01	15	8.1710E-02	7.4300E-02	2.5081E-01	2.5548E-01	2.7582E-01
20	2.9350E-02	2.0550E-02	3.5937E-01	3.6243E-01	4.3248E-01	20	2.7900E-03	1.6800E-03	2.2319E-01	2.2735E-01	2.3406E-01
30	8.3654E-01	8.6359E-01	2.9008E-01	2.9366E-01	2.9881E-01	30	1.5021E-01	1.8038E-01	5.3869E-01	5.3480E-01	5.4062E-01
40	3.7150E-02	4.7810E-02	5.9457E-01	5.8670E-01	5.8299E-01	40	9.7600E-03	1.0960E-02	1.2937E-01	1.2849E-01	1.1764E-01
60	1.6370E-02	1.4330E-02	9.6249E-01	9.6284E-01	9.5763E-01	60	2.3800E-02	2.4490E-02	8.9713E-01	8.9568E-01	8.9394E-01
90	2.7270E-02	3.3620E-02	6.8763E-01	6.8633E-01	6.5745E-01	90	4.0180E-02	4.4240E-02	7.1865E-01	7.1571E-01	7.1235E-01
120	1.9795E-01	1.9305E-01	3.7573E-01	3.7714E-01	4.0287E-01	120	2.6250E-01	2.4973E-01	2.6155E-01	2.6020E-01	2.6682E-01
150	6.7554E-01	6.6518E-01	3.0078E-01	3.1035E-01	4.4196E-01	150	7.1662E-01	7.0355E-01	6.2163E-01	6.2691E-01	6.2047E-01
179	9.0298E-01	8.7026E-01	9.8694E-01	9.8719E-01	9.8929E-01	179	3.4470E-02	4.7890E-02	9.8940E-01	9.8980E-01	9.8917E-01

available in the literature for comparison. Electron impact excitation lambda parameter results were also calculated for comparison purposes.

The lambda parameter results are characterized by fall and rise for all the distortion potentials as shown in figure 7. From the formula of calculating lambda, when  $\lambda \approx 1$ , then  $\sigma'_o(\theta, \phi) > \sigma'_1(\theta, \phi)$ . This shows that most of the particles are scattered from the magnetic sub-state  $m = 0$ . Also, when  $\lambda = 0.333$ , the particles are evenly scattered from the two magnetic sub-states. The oscillating behavior of the lambda parameter in relation to the scattering angle shows that the scattering of particles is alternating between the two magnetic sub-states

Lambda parameter results using static and absorption potentials have the same trend as the results when using static potential though there is a difference in magnitude at low impact energies. The inclusion of polarization potential greatly affects the magnitude of lambda parameter for different angles but the results are still characterized by fall and rise. The results using distortion potential with static, polarization, and absorption potentials have the same trend as the results when using static and polarization potentials. The effect of polarization potential shown in positron impact excitation results is also shown in the present electron impact excitation results. The electron impact excitation results have the same trend as the results of positron impact



excitation using distorting potential with static, absorption, and polarization potentials at all angles though there is a small variation at low impact energies.

## 4. Conclusion

In the present work, positron impact excitation cross-sections and angular correlation parameters for the lowest autoionizing state of potassium are calculated employing the quantum mechanical approach, the non-relativistic distorted wave method. The parameters are calculated for an extensive energy range from near excitation threshold to 1500 eV. The integral cross sections and alignment parameter results are in qualitative agreement with the only available results of Pangantiwar and Srivastava [21].

There are no previously reported experimental data for positron impact excitation of the autoionizing state of the potassium atom. However, a comparison with the Pangantiwar and Srivastava [21] positron impact results, present and experimental electron impact excitation results confirm the reliability of our results. Furthermore, the distorted wave method has been successfully applied with minimal computational cost to electron and positron scattering from different atomic and molecular systems in the past. This gives us confidence that the present study thus produces reliable data in the reported energy range.

However, the single configuration Hartree–Fock model used in this study is not highly accurate for the lowest states. Also, neglect of the contribution of the transitions from other excited states to the lowest autoionizing level of the potassium atom had our results have variation in magnitude at some energy regions in comparison with the experimental results. Despite the disparity in magnitude, our results are in quite good qualitative agreement with the electron impact excitation experimental results. Hence, our results can be relied on to giving guidance to future studies.

As discussed above, a sufficient amount of literature is available for electron impact excitation for alkali atoms, yet there is a rarity of data using positron impact excitation. In this study, the polarization potential used contains an adjustable parameter. Since the study was based on the understanding that the interaction potential can be chosen arbitrarily to reproduce reliable results, an adjustable parameter-free model can be considered in future studies. In view of this, a more rigorous theoretical and experimental effort is desirable for potassium to test the reliability of the presently reported data. Moreover, this is the first attempt to calculate cross-sections and angular correlation parameters for the lowest autoionizing state of the potassium atom using a complex distortion potential for such a wide energy range.

## Data availability statement

All data that support the findings of this study are included within the article (and any supplementary files).

## ORCID iDs

Noah Nzeki William  <https://orcid.org/0000-0001-5698-764X>

Eric Ouma Jobunga  <https://orcid.org/0000-0002-2998-7131>

Chandra Shekhar Singh  <https://orcid.org/0000-0002-7698-5817>

## References

- [1] Bray I, Fursa D V, Kadyrov A S, Lugovskoy A V, Savage J S, Stelbovics A T, Utamuratov R and Zammit M C 2014 Positron scattering on atoms and molecules *J. Phys. Conf. Ser.* **488** 012052
- [2] Kadyrov A S and Bray I 2016 Recent progress in the description of positron scattering from atoms using the convergent close-coupling theory *J. Phys. B: At. Mol. Opt. Phys.* **49** 222002
- [3] Ratnavelua K and Ong W E 2011 Electron and positron scattering from atomic potassium *Eur. Phys. J. D* **64** 269–85
- [4] Costello D G, Groce D E, Herring D F and McGowan J 1972 Evidence for the negative work function associated with positrons in gold *Phys. Rev. B* **5** 1433
- [5] Reid David D and Wadehra J M 1996 A quasi-free model for the absorption effects in positron scattering by atoms *Journal of Physics B Atomic, Molecular and Optical Physics* **29** L127–33
- [6] Surko C M, Gribakin G F and Buckman S J 2005 Low-energy positron interactions with atoms and molecules *J. Phys. B: At. Mol. Opt. Phys.* **38** R57–126
- [7] Salah Y E-B 2007 Elastic and inelastic scattering of positrons by potassium atoms *Mod. Phys. Lett. B* **21** 625–37
- [8] Nidhi S, Suvam S and Bobby A 2018 Positron total scattering cross-sections for alkali atoms *J. Phys. B: At. Mol. Opt. Phys.* **51** 015204
- [9] Burrows A and Volobuyev M 2003 Calculations of the far-wing line profiles of sodium and potassium in the atmosphere of substellar-mass objects *Astrophys. J.* **583** 985–95
- [10] Derek H, Nicole A and France A 2007 Alkali line profiles in degenerate dwarfs *AIP Conf. Proc.* **938** 170–5
- [11] Kariuki P K 2015 Comparison of the optical potential method and the distorted wave Born approximation method in electron—atom elastic scattering *PhD thesis* Kenyatta University (<http://ir-library.ku.ac.ke/handle/123456789/14249>)
- [12] Guessoum N, Ramaty R and Lingenfelter R 1991 Positron annihilation in the interstellar medium *Astrophys. J.* **378** 170–80
- [13] Murphy R J and Share G H 2005 The physics of positron annihilation in the solar atmosphere *Astrophys. J. Suppl. Ser.* **161** 495–519
- [14] Charlton M and Humberston J W 2001 *Positron Physics* (Cambridge: Cambridge University Press) (<https://doi.org/10.1017/CBO9780511535208>)
- [15] Pedersen T S, Danielson J R, Christoph H, Marx G, Xabier S, Schauer F, Schweikhard L, Surko C and Winkler E 2012 Plan for the creation and studies of electron-positron plasmas in a stellarator *New J. Phys.* **14** 035010 1–14
- [16] Saitoh H, Pedersen T S, Hergenhanh U, Stenson E V, Paschkowski N and Hugschmid C 2014 Recent status of a positron-electron experiment (apex) *Journal of Physics: Conference Series* **505** 012045
- [17] Wagner A, Anwand W, Butterling M, Fiedler F, Fritz F, Kempe M and Cowan T E 2014 Tomographic positron annihilation lifetime spectroscopy *J. Phys. Conf. Ser.* **505** 012034
- [18] Del Guerra A, Nicola B and Giuseppina M B 2016 Positron emission tomography: Its 65 years *La Rivista del Nuovo Cimento* **39** 155–223
- [19] Baró J, Sempau J, Fernández-Varea J M and Salvat F 1995 Penelope: an algorithm for monte Carlo simulation of the penetration and energy loss of electrons and positrons in matter *Nuclear Instruments and Methods in Physics Research Section B* **100** 31–46
- [20] Slaughter R, Davis A, Davis N, Szumila H, Smith D and Tiradani A 2007 Monte carlo analysis for positron annihilation rocketry using geant 4 *3rd AIAA/ASME/SAE/ASEE Joint Propulsion Conference & Exhibit AIAA 2007-5605* 1–8
- [21] Pangantiwar A and Srivastava R 1987  $e^{\pm}$  impact excitation of autoionizing levels in alkali: a distorted wave approach *J. Phys. B: At. Mol. Opt. Phys.* **20** 5881–902
- [22] Itikawa Y and Sakimoto K 1985 Distorted-wave-method calculation of electron-impact excitation of atomic ions: He- and be-like ions *Phys. Rev. A* **31** 1319–27
- [23] Itikawa Y 1986 Distorted-wave methods in electron-impact excitation of atoms and ion *Phys. Rep.* **143** 69–108
- [24] Katiyar K and Srivastava R 1988 Distorted wave calculation of the cross-sections and correlation parameter for  $e^{\pm}$  collisions *Phys. Rev. A* **38** 2767–81
- [25] Ward S J, Horbatsch M, McEachran R P and Stauffer A D 1988 Close-coupling approach to positron scattering for lithium, sodium and potassium *J. Phys. B: At. Mol. Opt. Phys.* **22** 1845–61
- [26] Madison H and Bartschart K 1996 The distorted wave method for elastic scattering and atomic excitation *Computational Atomic Physics* ed K Bartschart (Berlin: Springer) 65–85
- [27] Clementi E and Roetti C 1974 Roothan—Hartree -Fock atomic wave functions *At. Data Nucl. Data Tables* **14** 177–478
- [28] Joachain Charles Jean 1975 *Quantum Collision Theory* (Amsterdam: North-Holland Pub. Co) ([https://inis.iaea.org/search/search.aspx?orig\\_q=source:%22ISBN%200720402948%22](https://inis.iaea.org/search/search.aspx?orig_q=source:%22ISBN%200720402948%22))
- [29] Singh C S 2004 Magnetic-sublevel differential cross sections for electron-impact excitation of  $2^1P$  state of helium *East African Journal of Physical Sciences* **5** 85–98 (<https://ir-library.ku.ac.ke/handle/123456789/12878>)
- [30] Nahar S N and Wadehra J M 1986 Elastic scattering of positrons and electrons by argon *Phys. Rev. A* **35** 5
- [31] Staszewska G, Schwenke D W and Truhlar D G 1984 Investigation of the shape of the imaginary part of the optical-model potential for electron scattering by rare gases *Phys. Rev. A* **29** 6
- [32] Reid D D and Wadehra J M 1998 Intermediate- to high-energy positrons scattered by alkali-metal atoms *Phys. Rev. A* **57** 2583–9
- [33] Schwerdtfeger P and Nagle J 2019 2018 Table of static dipole polarizabilities of neutral elements in periodic table *Mol. Phys.* **117** 1200–25
- [34] Jobunga E O, Okumu J and Singh C S 2012 Excitation cross-section evaluation for the lowest auto-ionizing state of potassium *The African Review of Physics* **7** 0001 (<http://aphysrev.ictp.it/index.php/aphysrev/issue/view/28>)

- [35] Furness J B and McCarthy I E 1973 Semiphenomenological optical model for electron scattering on atoms *J. Phys. B: At. Mol. Opt. Phys.* **6** 2280–91
- [36] Saxena S and Mathur K C 1986 Study of angular correlation parameters in positron-lithium scattering *J. Phys. B: At. Mol. Opt. Phys.* **19** 3181–6
- [37] Morgan L A and McDowell M R C 1975 Electron impact excitation of H and  $\text{He}^+$ .iv. orientation and alignment of the 2p state *J. Phys. B: At. Mol. Opt. Phys.* **8** 1073–81
- [38] Kaur S and Srivastava R 1999 Excitation of the lowest autoionizing  $np^5(n.1)s^2,^2P_{3/2,1/2}$  states of Na ( $n = 2$ ), K( $n=3$ ), Rb ( $n = 4$ ) and Cs ( $n = 5$ ) by electron impact *J. Phys. B: At. Mol. Opt. Phys.* **32** 2323–42
- [39] Feuerstein B, Grum-Grzhimailo A N and Mehlhorn W 1999 Electron-impact excitation cross-sections of  $K^*(3p^54s^2,^2P_{3/2},^2P_{1/2})$  autoionizing states: strong fine-structure dependence near-threshold *J. Phys. B: At. Mol. Opt. Phys.* **32** 4547–54
- [40] Borovik A A, Grum-Grzhimailo A N, Bartschat K and Zatsarinny O 2005 Electron impact excitation of the  $(3p^54s^2)^2P_{3/2,1/2}$  autoionizing states in potassium *J. Phys. B: At. Mol. Opt. Phys.* **38** 1081–92
- [41] Grum-Grzhimailo A N and Bartschat K 2000 Excitation of the  $3p^54s^2p$  autoionizing state in potassium by electron impact at low energies: an r-matrix calculation *J. Phys. B: At. Mol. Opt. Phys.* **33** 1843–53
- [42] Stein T S, Harte M, Jiang W E, Kauppila J, Kwan C K, Li H and Zhou S 1998 Measurements of positron scattering by hydrogen, alkali metal, and other atoms *Nucl. Instrum. Methods Phys. Res. B* **143** 68–80
- [43] Matterstock B, Huster R, Paripast A N and Grum-Grzhimailo B 1995 and W. Mehlhorn. Excitation of  $K^*(3p^54s^2,^2P_{3/2},^2P_{1/2})$  by electron impact in the range from near-threshold to 500 ev: alignment and cross-section ratios *J. Phys. B: At. Mol. Opt. Phys.* **28** 4301–9